

# Changes in the structure, mechanical and corrosion properties of the Mg–Zn–Zr system alloy subjected to equal channel angular pressing

© 2024

Denis A. Aksenov<sup>\*1,2,3</sup>, junior researcher  
 Elvira I. Fakhretdinova<sup>1,2</sup>, PhD (Engineering), researcher  
 Rashid N. Asfandiyarov<sup>1,2,4</sup>, PhD (Engineering), researcher  
 Arseniy G. Raab<sup>2,5</sup>, PhD (Engineering), researcher  
 Arseniy E. Sharipov<sup>2</sup>, graduate student  
 Mariya A. Shishkunova<sup>2</sup>, postgraduate student  
 Yuliya R. Sementeeva<sup>2</sup>, graduate student

<sup>1</sup>Institute of Physics of Molecules and Crystals of Ufa Federal Research Center of RAS, Ufa (Russia)<sup>2</sup>Ufa University of Science and Technology, Ufa (Russia)

\*E-mail: aksyonovda@mail.ru

<sup>3</sup>ORCID: <https://orcid.org/0000-0002-2652-2646><sup>4</sup>ORCID: <https://orcid.org/0000-0002-5522-4314><sup>5</sup>ORCID: <https://orcid.org/0000-0003-1993-413X>

Received 05.06.2023

Accepted 25.08.2023

**Abstract:** Magnesium alloys are considered promising materials for the production of bioresorbable implants. Their main disadvantages are low strength and corrosion resistance in biological environment. In the work, the authors studied the effect of severe plastic deformation using the equal channel angular pressing (ECAP) method on the structure, mechanical properties, and corrosion resistance of the Mg–8.6Zn–1.2Zr magnesium alloy. It was identified that one ECAP cycle at 400 °C leads to a substantial hardening of the Mg–8.6Zn–1.2Zr alloy by ~10 %, up to 330 MPa. Structural studies showed that dynamic recrystallisation plays a significant role in the structure transformation. ECAP leads to the formation of a bimodal structure with large deformed grains with an average transverse size of 20±4 µm and recrystallised grains with an average transverse size of 6±2 µm. It was found that with a decrease in the strain temperature up to 250 °C, the process of deformation-induced decay of the supersaturated solid solution takes place. Electrical conductivity of a sample after ECAP at 400 °C amounted 29±2 % according to the International Annealed Copper Standard (IACS), while second ECAP cycles lead to an increase in the electrical conductivity up to 32±2 % IACS. Using the electrochemical corrosion method, the authors found that one ECAP cycle at 400 °C leads to a slight decrease in the corrosion resistance of the alloy under study compared to the initial state. The study showed that the corrosion current increases from 24 to 32 µA/cm<sup>2</sup>, while the subsequent ECAP cycle at 250 °C increases the corrosion current more than twice (up to 57 µA/cm<sup>2</sup>).

**Keywords:** Mg–Zn–Zr system alloys; Mg–8.6Zn–1.2Zr; magnesium alloys; high strength of magnesium alloys; ECAP; corrosion resistance; electrical conductivity; dynamic recrystallisation during ECAP.

**Acknowledgments:** The work was supported by the Russian Science Foundation (grant No. 22-79-10325, <https://www.rscf.ru/project/22-79-10325/>).

The paper was written on the reports of the participants of the XI International School of Physical Materials Science (SPM-2023), Togliatti, September 11–15, 2023.

**For citation:** Aksenov D.A., Fakhretdinova E.I., Asfandiyarov R.N., Raab A.G., Sharipov A.E., Shishkunova M.A., Sementeeva Yu.R. Changes in the structure, mechanical and corrosion properties of the Mg–Zn–Zr system alloy subjected to equal channel angular pressing. *Frontier Materials & Technologies*, 2024, no. 1, pp. 9–17. DOI: 10.18323/2782-4039-2024-1-67-1.

## INTRODUCTION

Currently, magnesium alloys are considered as promising materials for the development and production of biodegradable implants, to use in traumatology and surgery [1–3]. The attention was paid to these alloys for a good reason: magnesium has an elastic modulus close to human bone; it is non-toxic and biocompatible with the human body [4]. However, for the full use of these materials, it is necessary to eliminate a number of their demerits, first, to increase the strength characteristics. Alloying is one of the ways to solve this problem. Magnesium itself has a low capacity for strain hardening, but alloying can increase the hardening effect during thermomechanical processing. In particular, widespread

magnesium systems with zinc and zirconium can be selected. Due to solid solution strengthening in Mg–Zn systems, the strength increases, and additional alloying with zirconium allows increasing ductility [5–7]. For magnesium alloys, processes of multi-cycle rolling with decreasing temperature are widespread [8]. As a result of this processing, products with high strength are produced due to the formation of a lineage and partially recrystallised structure. One should, note that the high extent of the boundaries of deformed grains, and the high dislocation density in this case can negatively affect the corrosion resistance of magnesium alloys [9–11].

Researchers have also drawn attention to methods based on the principles of severe plastic deformation. It is shown in [12–14] that high-pressure torsion can lead to

more efficient refinement of the structure of magnesium materials compared to rolling, however, this deformation method is not scalable. Another approach is equal channel angular pressing (ECAP). As a rule, to achieve strength above 300 MPa, from 2 to 4 deformation treatment cycles are carried out [15–17]. In this case, the effect of sliding along the main base plane has been identified, which reduces the ECAP effectiveness, and in some cases even leads to softening of the material with an increase in the number of deformation cycles [18–20]. However, thermomechanical processing, including ECAP and carried out according to special technological modes, can achieve the required set of properties.

The purpose of this work is to determine the influence of the deformation mode during equal channel angular pressing (ECAP) on the features of the structural state formation, corrosion resistance and mechanical characteristics of the Mg–Zn–Zr system alloy.

## METHODS

The magnesium Mg–8.6Zn–1.2Zr (wt. %) alloy was chosen as the research material. Chemical analysis was carried out on a Thermo Scientific ARL Optim'X X-ray fluorescence spectrometer. The material as-delivered is a strip 20 mm thick, from which samples with a diameter of 20 mm, and a length of 100 mm were cut along the rolling direction on an ARTA-120 spark-cutting mill.

The initial state was taken to be after prolonged annealing at 400 °C for 24 h. The mode was chosen based on literature data [21–23] and state diagrams of the Mg–Zn and Mg–Zr systems. Annealing was carried out in air in a Snol 8.2/1000 furnace with air cooling.

Deformation processing using the ECAP method was carried out in 2 regimes.

1. Initial temperature of equipment and blanks is 400 °C, channel intersection angle is 120°, and deformation rate is 1 mm/s, 1 cycle.

2. Processing according to mode 1, then 1 ECAP cycle according to Bc route (the blank was turned around 90° relative to the longitudinal axis), at an initial temperature of the equipment and blanks of 250 °C, the channel intersection angle of 90°, the deformation rate of 1 mm/s, in copper shell 1.5 mm thick.

Structural studies were performed using an Olympus GX51 light microscope and a JSM6490 scanning electron microscope.

Mechanical tests were carried out in accordance with GOST 1497-84. For tensile tests, proportional cylindrical samples with a working part diameter of 3 mm and an initial gauge length of 15 mm were used. Tests were performed on an Instron 5982 electromechanical static test system, at room temperature, at a rate of 1 mm/min.

Electrical conductivity was determined using a VE-27NTs eddy-current meter, converting the obtained values into IACS (International Annealed Copper Standard).

Electrochemical corrosion tests were carried out using an Elins R-5X potentiostat-galvanostat-impedancemeter in Ringer's solution with pH=7.4 in a three-electrode 80 ml cell with a silver chloride reference electrode and a platinum counter electrode. The tests were carried out at a temperature of 37 °C for 12 h, while during the first 2 h

the electrode free corrosion potential was measured until a steady state was established on the surface of the sample. To obtain polarisation curves after establishing a steady state, a potential sweep was performed in the range from –300 to +300 mV relative to the steady-state value of the electrode potential with a scanning velocity of 0.25 mV/s. The current and corrosion potential were calculated from polarisation curves using Tafel sections [24].

## RESULTS

In the initial heat-treated state, the Mg–8.6Zn–1.2Zr alloy sample has a coarse-grained state with a bimodal grain size distribution (Fig. 1). Large grains with an average transverse size of 30±10 µm and small recrystallised grains with an average transverse size of 4±2 µm are observed. The initial state can be additionally characterised by such a structure-sensitive parameter as electrical conductivity, which helps to assess indirectly, the change in the solid solution concentration in the alloy during further deformation processing. In the initial state, the electrical conductivity was 29±2 % IACS.

As a result of deformation processing carried out in regimes 1 and 2, it was identified that the structure bimodal appearance was preserved in the samples (Fig. 2). After 1 ECAP cycle, the deformation texture is clearly pronounced, coarse grains are turned in the direction of shear action in the ECAP focus, their average transverse size decreased to 20±4 µm, recrystallised grains have an average transverse size of 6±2 µm and are located mainly along the boundaries of large deformed grains. This indicates the implementation of processes of both grain transformation and dynamic recrystallisation. The second cycle in regime 2 does not make significant changes to the nature of the structure. Coarse deformed grains with an average transverse size of 18±4 µm and recrystallised grains with an average transverse size of 5±2 µm are observed.

After deformation in regime 1, the electrical conductivity remained at the level of 29±2 % IACS. After deformation in regime 2, it was 32±2 % IACS. This change is most likely explained by temperature conditions.

The results of mechanical tensile tests indicate an increase in the Mg–8.6Zn–1.2Zr alloy strength after ECAP (Fig. 3). After the 1<sup>st</sup> ECAP cycle, the tensile strength increased from 300±7 to 330±5 MPa; the 2<sup>nd</sup> cycle did not lead to an increase in strength.

The next important characteristic of the material for the production of implants is its corrosion resistance. From the analysis of the obtained results of corrosion tests presented in the form of polarisation curves, the values of the corrosion current ( $i_{corr}$ ) and free corrosion potential ( $E_{corr}$ ) were obtained (Table 1). Fig. 4 shows that Tafel regions are observed on the cathode branches of the samples. As a result of ECAP treatment in regimes 1 and 2, the surfaces of the samples are passivated, as evidenced by the lower value of the free corrosion potential  $E_{corr}$ . Based on the results presented in Table 1, the initial sample with the minimum corrosion current  $i_{corr}$  has the best corrosion properties. The displacement of the cathodic branches indicates a change in the surface area available for the cathodic reaction.

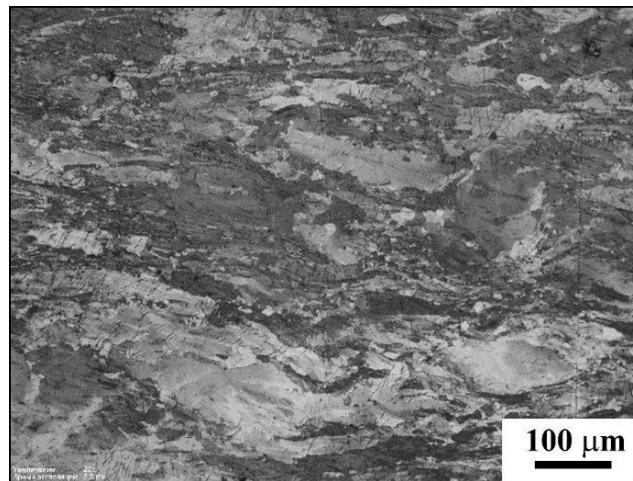


**Fig. 1.** The structure of the Mg–Zn–Zr system alloy after annealing at 400 °C for 24 h. Light microscopy  
**Рис. 1.** Структура сплава системы Mg–Zn–Zr после отжига при 400 °C в течение 24 ч. Световая микроскопия

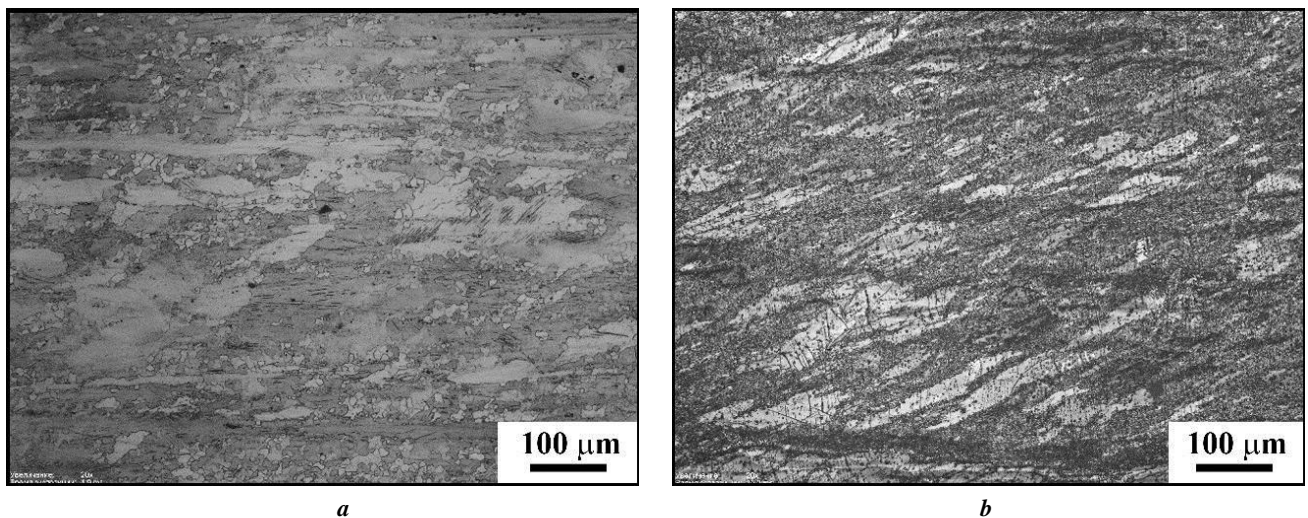


**Fig. 2.** The structure of the Mg–Zn–Zr system alloy after ECAP according to regimes 1 (a) and 2 (b)  
**Рис. 2.** Структура сплава системы Mg–Zn–Zr после РКВИ по режиму 1 (a) и 2 (b)

## DISCUSSION

The strength properties, and corrosion resistance of a magnesium alloy are closely related to its structural state. Structure refinement can have a dual effect on the corrosion resistance of magnesium alloys. With the Mg–Al system, grinding will lead to an increase in corrosion resistance [25], while for a Mg–Zn–Zr system alloy, the nature of the corrosion behaviour may be different, due to the type and distribution of the second phase dispersed particles along the grain boundaries, and therefore an increase in the corrosion rate is possible [26]. The results of measuring electrical conductivity can indirectly prove the change in the solid solution concentration and the process of precipitation of the second phase particles. It is known that at temperatures above 300 °C, the solubility of both Zn and Zr increases. Thus, ECAP at 250 °C leads to the decomposition of the solid solution of alloying elements.

It was found that in regime 1, when the temperature was 400 °C, the electrical conductivity corresponded to the value of the annealed state of 29 % IACS. Regime 2 at a temperature of 250 °C leads to an increase in the material electrical conductivity up to 32 % IACS. Thus, lowering the deformation processing temperature to 250 °C will lead to deformation-stimulated decomposition of the solid solution.

Electrochemical tests for corrosion resistance indicate that the magnesium alloy sample in the annealed state is of greatest importance, which is caused by the equilibrium state of the grain boundaries [27]. A decrease in the average transverse size of coarse and recrystallised grains, texturing, and the possible increase in the number of crystal lattice defects, as well as a change in the solid solution state, lead to an increase in corrosion currents. Moreover, after high-temperature deformation processing in regime 1,

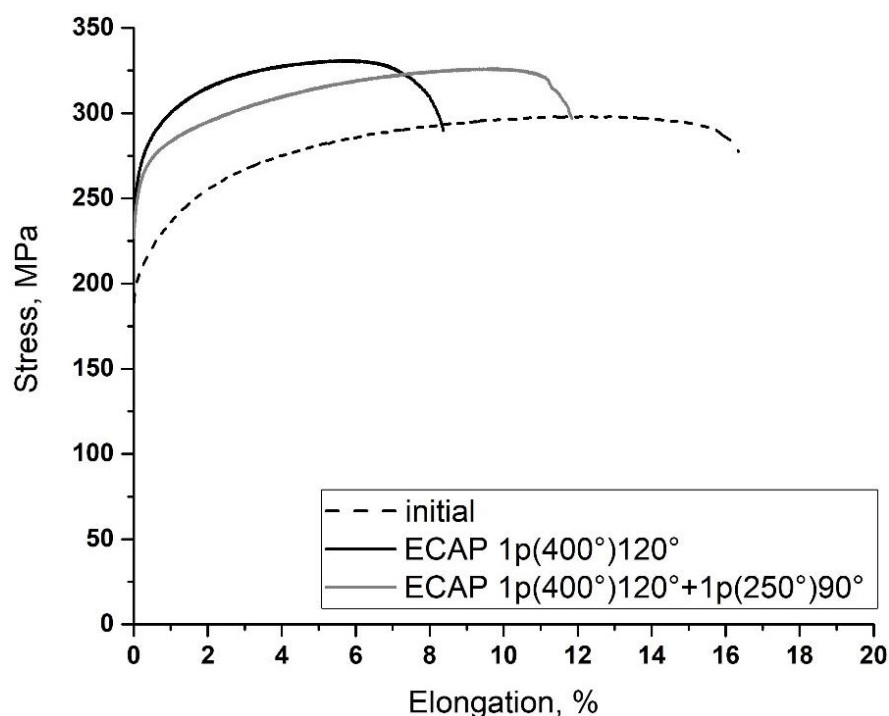


**Fig. 3.** Curves of mechanical tests of the Mg–Zn–Zr system alloy after annealing at 400 °C, ECAP according to regimes 1 and 2  
**Рис. 3.** Кривые механических испытаний сплава системы Mg–Zn–Zr после отжига при 400 °C, РКУП по режимам 1 и 2

**Table 1.** Values of corrosion current and free corrosion potential  
**Таблица 1.** Значения тока коррозии и потенциала свободной коррозии

State	$I_{corr}, \mu\text{A}/\text{cm}^2$	$E_{corr}, \text{V}$
Initial state (400 °C, 24 h)	24.05±5.46	-1.428±0.013
ECAP, regime 1	32.06±16.20	-1.382±0.030
ECAP, regime 2	57.00±6.22	-1.391±0.085

the increase is ~25 %, and after the 2<sup>nd</sup> cycle of deformation at a lower temperature (250 °C) in accordance with regime 2, the corrosion current increases by more than 2 times relative to the initial state. One should note that on the Mg–8.6Zn–1.2Zr alloy, it was possible to achieve high values of ultimate strength and offset yield strength within just one ECAP cycle. Table 2 presents a comparison of the achieved strength characteristics with the results of other studies on the alloys of similar chemical composition.

## CONCLUSIONS

It was identified that during ECAP deformation processing of the Mg–8.6Zn–1.2Zr alloy, temperature plays a significant role. Thus, at 400 °C, the main mechanism of structure formation during deformation is dynamic recrystallisation, while the solid solution state is maintained.

Deformation processing of the Mg–8.6Zn–1.2Zr alloy by ECAP, 1 cycle, channel intersection angle 120°, 400 °C (mode 1), leads to the formation of a structure with recrystallised grains with an average transverse size of 6±2 µm, and larger deformed grains directed along the shear direction, with an average transverse size of 20±4 µm. Such structural state provides an increase in tensile strength relative to the initial one annealed by ~10 %, up to 330 MPa.

Electrical conductivity measurements, indirectly indicate that lowering the temperature of ECAP deformation processing to 250 °C leads to deformation-induced decomposition of the supersaturated solid solution. The electrical conductivity after deformation in regime 1 was 29±2 % IACS, while the final electrical conductivity after deformation of the Mg–8.6Zn–1.2Zr alloy in regime 2 differs from the initial state by 3 % and amounts to 32±2 % IACS.

**Table 2.** Mechanical characteristics of the Mg–Zn–Zr system alloy after ECAP  
**Таблица 2.** Механические характеристики сплава системы Mg–Zn–Zr после РКВП

Work	Mode	UTS, MPa	YTS, MPa	Percentage elongation, %
Current work	ECAP, regime 1	330	267	8
	ECAP, regime 2	325	245	12
[16]	4 ECAP cycles, Bc route, 220 °C, channel intersection angle 90°	290	231	27
[28]	2 ECAP cycles, Bc route, channel intersection angle 90°	341	264	23
	4 ECAP cycles, Bc route, 220 °C, channel intersection angle 90°	334	277	21
[29]	2 ECAP cycles, 250 °C, channel intersection angle 90°	326	175	25

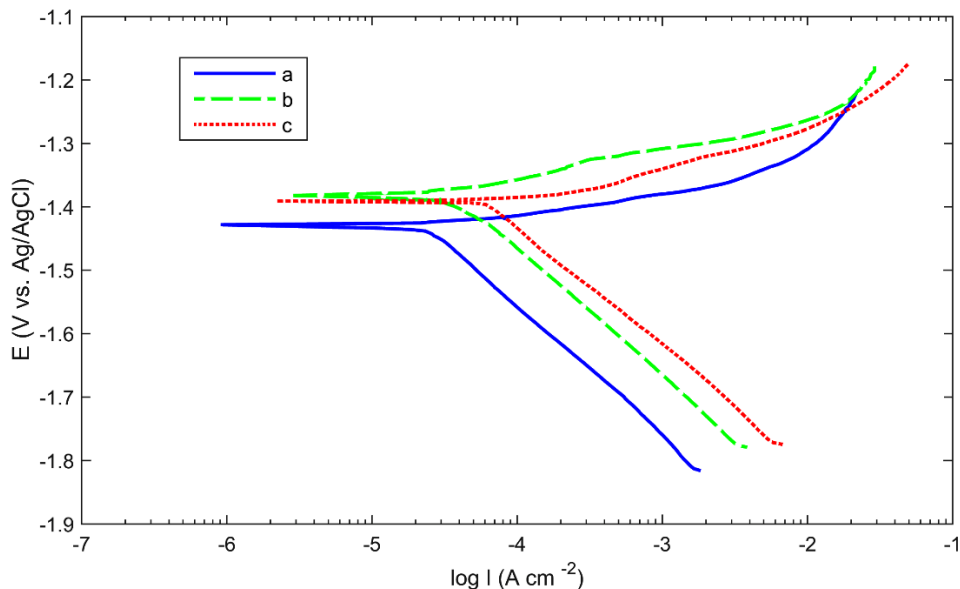


**Fig. 4.** Polarisation curves: a – initial state; b – regime 1; c – regime 2  
**Рис. 4.** Поляризационные кривые: a – исходное состояние; b – режим 1; c – режим 2

The results of electrochemical corrosion tests indicate that the magnesium alloy sample in the initial annealed state, has the greatest resistance to corrosion. 1 ECAP cycle at 400 °C leads to an increase in the corrosion current by 25 % ( $32.06 \pm 16.20 \mu\text{A}/\text{cm}^2$ ), while subsequent deformation at 250 °C leads to an increase in the corrosion current by more than 2 times ( $57.00 \pm 6.22 \mu\text{A}/\text{cm}^2$ ).

**REFERENCES**

1. Li N., Zheng Y. Novel Magnesium Alloys Developed for Biomedical Application: A Review. *Journal of Mate-*

*rials Science and Technology*, 2013, vol. 29, no. 6, pp. 489–502. DOI: [10.1016/j.jmst.2013.02.005](https://doi.org/10.1016/j.jmst.2013.02.005).  
 2. Chen Y., Xu Z., Smith C., Sankar J. Recent advances on the development of magnesium alloys for biodegradable implants. *Acta Biomaterialia*, 2014, vol. 10, no. 11, pp. 4561–4573. DOI: [10.1016/j.actbio.2014.07.005](https://doi.org/10.1016/j.actbio.2014.07.005).  
 3. Gu X.-N., Zheng Y.-F. A review on magnesium alloys as biodegradable materials. *Frontiers of Materials Science in China*, 2010, vol. 4, pp. 111–115. DOI: [10.1007/s11706-010-0024-1](https://doi.org/10.1007/s11706-010-0024-1).  
 4. Saris N.-E.L., Mervaala E., Karppanen H., Khawaja J.A., Lewenstam A. Magnesium: An update on physiological,



- clinical and analytical aspects. *Clinica Chimica Acta*, 2000, vol. 294, no. 1-2, pp. 1–26. DOI: [10.1016/S0009-8981\(99\)00258-2](https://doi.org/10.1016/S0009-8981(99)00258-2).
5. Yin D., Zhang E., Zeng S. Effect of Zn on mechanical property and corrosion property of extruded Mg-Zn-Mn alloy. *Transactions of Nonferrous Metals Society of China*, 2008, vol. 18, no. 4, pp. 763–768. DOI: [10.1016/S1003-6326\(08\)60131-4](https://doi.org/10.1016/S1003-6326(08)60131-4).
  6. Cai S., Lei T., Li N., Feng F. Effects of Zn on microstructure, mechanical properties and corrosion behavior of Mg-Zn alloys. *Materials Science and Engineering: C*, 2012, vol. 32, no. 8, pp. 2570–2577. DOI: [10.1016/j.msec.2012.07.042](https://doi.org/10.1016/j.msec.2012.07.042).
  7. Zhao T., Hu Y., Pan F., He B., Guan M., Yuan Y., Tang A. Effect of Zn Content on the Microstructure and Mechanical Properties of Mg-Al-Sn-Mn Alloys. *Materials*, 2019, vol. 12, no. 19, article number 3102. DOI: [10.3390/ma12193102](https://doi.org/10.3390/ma12193102).
  8. Bohlen J., Kurz G., Yi S., Letzig D. Rolling of magnesium alloys. *Advances in Wrought Magnesium Alloys*. Sawston, Woodhead Publishing Limited, 2012, pp. 346–375.
  9. Xin R., Li B., Li L., Liu Q. Influence of texture on corrosion rate of AZ31 Mg alloy in 3.5wt.% NaCl. *Materials & Design*, 2011, vol. 32, no. 8-9, pp. 4548–4552.
  10. Zheng F., Chen H., Zhang Y., Wang W., Nie H. Microstructure evolution and corrosion resistance of AZ31 magnesium alloy tube by stagger spinning. *International Journal of Minerals, Metallurgy and Materials*, 2022, vol. 29, pp. 1361–1372. DOI: [10.1007/s12613-021-2396-x](https://doi.org/10.1007/s12613-021-2396-x).
  11. Sun J., Zhao W., Yan P., Chen K., Jiao L., Qiu T., Wang X. Effect of Corrosive Medium and Surface Defect-Energy on Corrosion Behavior of Rolled ZK61M Alloy. *Materials*, 2022, vol. 15, no. 12, article number 4091. DOI: [10.3390/ma15124091](https://doi.org/10.3390/ma15124091).
  12. Li W., Liu X., Zheng Y. et al. In vitro and in vivo studies on ultrafine-grained biodegradable pure Mg, Mg-Ca alloy and Mg-Sr alloy processed by high-pressure torsion. *Biomaterials Science*, 2020, no. 18, pp. 5071–5078. DOI: [10.1039/D0BM00805B](https://doi.org/10.1039/D0BM00805B).
  13. Medeiros M.P., Carvalho A.P., Isaac A., Afonso C.R.M., Janeček M., Minárik P., Celis M.M., Figueiredo R.B. Using high pressure torsion to process magnesium alloys for biological applications. *Journal of Materials Research and Technology*, 2023, vol. 22, pp. 3075–3084. DOI: [10.1016/j.jmrt.2022.12.127](https://doi.org/10.1016/j.jmrt.2022.12.127).
  14. Yan Z., Zhu J., Zhang Z., Wang Q., Xue Y. The microstructural, textural, and mechanical effects of high-pressure torsion processing on Mg alloys: A review. *Frontiers in Materials*, 2022, vol. 9, article number 964992. DOI: [10.3389/fmats.2022.964992](https://doi.org/10.3389/fmats.2022.964992).
  15. Merson D., Brilevsky A., Myagkikh P., Tarkova A., Prokhorikhin A., Kretov E., Frolova T., Vinogradov A. The Functional Properties of Mg-Zn-X Biodegradable Magnesium Alloys. *Materials*, 2020, vol. 13, no. 3, article number 544. DOI: [10.3390/ma13030544](https://doi.org/10.3390/ma13030544).
  16. Yin D.L., Cui H.L., Qiao J., Zhang J.F. Enhancement of mechanical properties in a Mg-Zn-Zr alloy by equal channel angular pressing at warm temperature. *Materials Research Innovations*, 2015, vol. 19, no. 9, pp. 9–28. DOI: [10.1179/1432891715Z.0000000001912](https://doi.org/10.1179/1432891715Z.0000000001912).
  17. Vinogradov A., Vasilev E., Kopylov V.I., Linderov M., Brilevsky A., Merson D. High Performance Fine-Grained Biodegradable Mg-Zn-Ca Alloys Processed by Severe Plastic Deformation. *Metals*, 2019, vol. 9, no. 2, article number 186. DOI: [10.3390/met9020186](https://doi.org/10.3390/met9020186).
  18. Jahadi R., Sedighi M., Jahed H. ECAP effect on the micro-structure and mechanical properties of AM30 magnesium alloy. *Materials Science and Engineering: A*, 2014, vol. 593, pp. 178–184. DOI: [10.1016/j.msea.2013.11.042](https://doi.org/10.1016/j.msea.2013.11.042).
  19. Straumal B., Martynenko N., Temralieva D. et al. The Effect of Equal-Channel Angular Pressing on Microstructure, Mechanical Properties, and Biodegradation Behavior of Magnesium Alloyed with Silver and Gadolinium. *Crystals*, 2020, vol. 10, no. 10, article number 918. DOI: [10.3390/cryst10100918](https://doi.org/10.3390/cryst10100918).
  20. Gopi K.R., Shivananda Nayaka H. Microstructure and mechanical properties of magnesium alloy processed by equal channel angular pressing (ECAP). *Materials Today: Proceedings*, 2017, vol. 4, no. 9, pp. 10288–10292. DOI: [10.1016/j.matpr.2017.06.366](https://doi.org/10.1016/j.matpr.2017.06.366).
  21. Chen M., Ma C., Liu Q., Cheng M., Wang H., Hu X. Plastic Deformation Mechanism of High Strength and Toughness ZK61 Magnesium Alloy Plate by Multipass Horizontal Continuous Rolling. *Materials*, 2023, vol. 16, no. 3, article number 1320. DOI: [10.3390/ma16031320](https://doi.org/10.3390/ma16031320).
  22. Alawad M.O., Alateyah A.I., El-Garaihy W.H., BaQais A., Elkhatny S., Kouta H., Kamel M., El-Sanabary S. Optimizing the ECAP Parameters of Biodegradable Mg-Zn-Zr Alloy Based on Experimental, Mathematical Empirical, and Response Surface Methodology. *Materials*, 2022, vol. 15, no. 21, article number 7719. DOI: [10.3390/ma15217719](https://doi.org/10.3390/ma15217719).
  23. Choi H.Y., Kim W.J. Effect of thermal treatment on the bio-corrosion and mechanical properties of ultrafine-grained ZK60 magnesium alloy. *Journal of the Mechanical Behavior of Biomedical Materials*, 2015, vol. 51, pp. 291–301. DOI: [10.1016/j.jmbbm.2015.07.019](https://doi.org/10.1016/j.jmbbm.2015.07.019).
  24. Scully J.R. Polarization resistance method for determination of instantaneous corrosion rates. *Corrosion*, 2000, vol. 56, no. 2, pp. 199–218. DOI: [10.5006/1.3280536](https://doi.org/10.5006/1.3280536).
  25. Aung N.N., Zhou W. Effect of grain size and twins on corrosion behaviour of AZ31B magnesium alloy. *Corrosion Science*, 2010, vol. 52, no. 2, pp. 589–594. DOI: [10.1016/j.corsci.2009.10.018](https://doi.org/10.1016/j.corsci.2009.10.018).
  26. Zeng R., Kainer K.U., Blawert C., Dietzel W. Corrosion of an extruded magnesium alloy ZK60 component—The role of microstructural features. *Journal of Alloys and Compounds*, 2011, vol. 509, no. 13, pp. 4462–4469. DOI: [10.1016/j.jallcom.2011.01.116](https://doi.org/10.1016/j.jallcom.2011.01.116).
  27. Shang B., Lei L., Wang X., He P., Yuan X., Dai W., Li J., Jiang Y., Sun Y. Effects of grain boundary characteristics changing with cold rolling deformation on intergranular corrosion resistance of 443 ultra-pure ferritic stainless steel. *Corrosion Communications*,

- 2022, vol. 8, pp. 27–39. DOI: [10.1016/j.corcom.2022.07.002](https://doi.org/10.1016/j.corcom.2022.07.002).
28. Yan J., Qin Z., Yan K. Mechanical properties and microstructure evolution of Mg-6 wt%Zn alloy during equal-channel angular pressing. *Metals*, 2018, vol. 8, no. 10, article number 841. DOI: [10.3390/met8100841](https://doi.org/10.3390/met8100841).
  29. Dumitru F.-D., Higuera-Cobos O.F., Cabrera J.M. ZK60 alloy processed by ECAP: Microstructural, physical and mechanical characterization. *Materials Science and Engineering: A*, 2014, vol. 594, pp. 32–39. DOI: [10.1016/j.msea.2013.11.050](https://doi.org/10.1016/j.msea.2013.11.050).
- ### СПИСОК ЛИТЕРАТУРЫ
1. Li N., Zheng Y. Novel Magnesium Alloys Developed for Biomedical Application: A Review // *Journal of Materials Science and Technology*. 2013. Vol. 29. № 6. P. 489–502. DOI: [10.1016/j.jmst.2013.02.005](https://doi.org/10.1016/j.jmst.2013.02.005).
  2. Chen Y., Xu Z., Smith C., Sankar J. Recent advances on the development of magnesium alloys for biodegradable implants // *Acta Biomaterialia*. 2014. Vol. 10. № 11. P. 4561–4573. DOI: [10.1016/j.actbio.2014.07.005](https://doi.org/10.1016/j.actbio.2014.07.005).
  3. Gu X.-N., Zheng Y.-F. A review on magnesium alloys as biodegradable materials // *Frontiers of Materials Science in China*. 2010. Vol. 4. P. 111–115. DOI: [10.1007/s11706-010-0024-1](https://doi.org/10.1007/s11706-010-0024-1).
  4. Saris N.-E.L., Mervaala E., Karppanen H., Khawaja J.A., Lewenstam A. Magnesium: An update on physiological, clinical and analytical aspects // *Clinica Chimica Acta*. 2000. Vol. 294. № 1-2. P. 1–26. DOI: [10.1016/S0009-8981\(99\)00258-2](https://doi.org/10.1016/S0009-8981(99)00258-2).
  5. Yin D., Zhang E., Zeng S. Effect of Zn on mechanical property and corrosion property of extruded Mg-Zn-Mn alloy // *Transactions of Nonferrous Metals Society of China*. 2008. Vol. 18. № 4. P. 763–768. DOI: [10.1016/S1003-6326\(08\)60131-4](https://doi.org/10.1016/S1003-6326(08)60131-4).
  6. Cai S., Lei T., Li N., Feng F. Effects of Zn on microstructure, mechanical properties and corrosion behavior of Mg-Zn alloys // *Materials Science and Engineering: C*. 2012. Vol. 32. № 8. P. 2570–2577. DOI: [10.1016/j.msec.2012.07.042](https://doi.org/10.1016/j.msec.2012.07.042).
  7. Zhao T., Hu Y., Pan F., He B., Guan M., Yuan Y., Tang A. Effect of Zn Content on the Microstructure and Mechanical Properties of Mg-Al-Sn-Mn Alloys // *Materials*. 2019. Vol. 12. № 19. Article number 3102. DOI: [10.3390/ma12193102](https://doi.org/10.3390/ma12193102).
  8. Bohlen J., Kurz G., Yi S., Letzig D. Rolling of magnesium alloys // *Advances in Wrought Magnesium Alloys*. Sawston: Woodhead Publishing Limited, 2012. P. 346–375.
  9. Xin R., Li B., Li L., Liu Q. Influence of texture on corrosion rate of AZ31 Mg alloy in 3.5wt.% NaCl // *Materials & Design*. 2011. Vol. 32. № 8-9. P. 4548–4552.
  10. Zheng F., Chen H., Zhang Y., Wang W., Nie H. Microstructure evolution and corrosion resistance of AZ31 magnesium alloy tube by stagger spinning // *International Journal of Minerals, Metallurgy and Materials*. 2022. Vol. 29. P. 1361–1372. DOI: [10.1007/s12613-021-2396-x](https://doi.org/10.1007/s12613-021-2396-x).
  11. Sun J., Zhao W., Yan P., Chen K., Jiao L., Qiu T., Wang X. Effect of Corrosive Medium and Surface Defect-Energy on Corrosion Behavior of Rolled ZK61M Alloy // *Materials*. 2022. Vol. 15. № 12. Article number 4091. DOI: [10.3390/ma15124091](https://doi.org/10.3390/ma15124091).
  12. Li W., Liu X., Zheng Y. et al. In vitro and in vivo studies on ultrafine-grained biodegradable pure Mg, Mg-Ca alloy and Mg-Sr alloy processed by high-pressure torsion // *Biomaterials Science*. 2020. № 18. P. 5071–5078. DOI: [10.1039/D0BM00805B](https://doi.org/10.1039/D0BM00805B).
  13. Medeiros M.P., Carvalho A.P., Isaac A., Afonso C.R.M., Janeček M., Minárik P., Celis M.M., Figueiredo R.B. Using high pressure torsion to process magnesium alloys for biological applications // *Journal of Materials Research and Technology*. 2023. Vol. 22. P. 3075–3084. DOI: [10.1016/j.jmrt.2022.12.127](https://doi.org/10.1016/j.jmrt.2022.12.127).
  14. Yan Z., Zhu J., Zhang Z., Wang Q., Xue Y. The microstructural, textural, and mechanical effects of high-pressure torsion processing on Mg alloys: A review // *Frontiers in Materials*. 2022. Vol. 9. Article number 964992. DOI: [10.3389/fmats.2022.964992](https://doi.org/10.3389/fmats.2022.964992).
  15. Merson D., Brilevsky A., Myagkikh P., Tarkova A., Prokhorikhin A., Kretov E., Frolova T., Vinogradov A. The Functional Properties of Mg-Zn-X Biodegradable Magnesium Alloys // *Materials*. 2020. Vol. 13. № 3. Article number 544. DOI: [10.3390/ma13030544](https://doi.org/10.3390/ma13030544).
  16. Yin D.L., Cui H.L., Qiao J., Zhang J.F. Enhancement of mechanical properties in a Mg-Zn-Zr alloy by equal channel angular pressing at warm temperature // *Materials Research Innovations*. 2015. Vol. 19. № 9. P. 9–28. DOI: [10.1179/1432891715Z.0000000001912](https://doi.org/10.1179/1432891715Z.0000000001912).
  17. Vinogradov A., Vasilev E., Kopylov V.I., Linderov M., Brilevsky A., Merson D. High Performance Fine-Grained Biodegradable Mg-Zn-Ca Alloys Processed by Severe Plastic Deformation // *Metals*. 2019. Vol. 9. № 2. Article number 186. DOI: [10.3390/met9020186](https://doi.org/10.3390/met9020186).
  18. Jahadi R., Sedighi M., Jahed H. ECAP effect on the micro-structure and mechanical properties of AM30 magnesium alloy // *Materials Science and Engineering: A*. 2014. Vol. 593. P. 178–184. DOI: [10.1016/j.msea.2013.11.042](https://doi.org/10.1016/j.msea.2013.11.042).
  19. Straumal B., Martynenko N., Temralieva D. et al. The Effect of Equal-Channel Angular Pressing on Microstructure, Mechanical Properties, and Biodegradation Behavior of Magnesium Alloyed with Silver and Gadolinium // *Crystals*. 2020. Vol. 10. № 10. Article number 918. DOI: [10.3390/cryst10100918](https://doi.org/10.3390/cryst10100918).
  20. Gopi K.R., Shivananda Nayaka H. Microstructure and mechanical properties of magnesium alloy processed by equal channel angular pressing (ECAP) // *Materials Today: Proceedings*. 2017. Vol. 4. № 9. P. 10288–10292. DOI: [10.1016/j.matpr.2017.06.366](https://doi.org/10.1016/j.matpr.2017.06.366).
  21. Chen M., Ma C., Liu Q., Cheng M., Wang H., Hu X. Plastic Deformation Mechanism of High Strength and Toughness ZK61 Magnesium Alloy Plate by Multipass Horizontal Continuous Rolling // *Materials*. 2023. Vol. 16. № 3. Article number 1320. DOI: [10.3390/ma16031320](https://doi.org/10.3390/ma16031320).
  22. Alawad M.O., Alateyah A.I., El-Garaihy W.H., BaQais A., Elkhatny S., Kouta H., Kamel M., El-Sanabary S.

- Optimizing the ECAP Parameters of Biodegradable Mg–Zn–Zr Alloy Based on Experimental, Mathematical Empirical, and Response Surface Methodology // *Materials*. 2022. Vol. 15. № 21. Article number 7719. DOI: [10.3390/ma15217719](https://doi.org/10.3390/ma15217719).
23. Choi H.Y., Kim W.J. Effect of thermal treatment on the bio-corrosion and mechanical properties of ultrafine-grained ZK60 magnesium alloy // *Journal of the Mechanical Behavior of Biomedical Materials*. 2015. Vol. 51. P. 291–301. DOI: [10.1016/j.jmbbm.2015.07.019](https://doi.org/10.1016/j.jmbbm.2015.07.019).
24. Scully J.R. Polarization resistance method for determination of instantaneous corrosion rates // *Corrosion*. 2000. Vol. 56. № 2. P. 199–218. DOI: [10.5006/1.3280536](https://doi.org/10.5006/1.3280536).
25. Aung N.N., Zhou W. Effect of grain size and twins on corrosion behaviour of AZ31B magnesium alloy // *Corrosion Science*. 2010. Vol. 52. № 2. P. 589–594. DOI: [10.1016/j.corsci.2009.10.018](https://doi.org/10.1016/j.corsci.2009.10.018).
26. Zeng R., Kainer K.U., Blawert C., Dietzel W. Corrosion of an extruded magnesium alloy ZK60 component – the role of microstructural features // *Journal of Alloys and Compounds*. 2011. Vol. 509. № 13. P. 4462–4469. DOI: [10.1016/j.jallcom.2011.01.116](https://doi.org/10.1016/j.jallcom.2011.01.116).
27. Shang B., Lei L., Wang X., He P., Yuan X., Dai W., Li J., Jiang Y., Sun Y. Effects of grain boundary characteristics changing with cold rolling deformation on intergranular corrosion resistance of 443 ultra-pure ferritic stainless steel // *Corrosion Communications*. 2022. Vol. 8. P. 27–39. DOI: [10.1016/j.corcom.2022.07.002](https://doi.org/10.1016/j.corcom.2022.07.002).
28. Yan J., Qin Z., Yan K. Mechanical properties and microstructure evolution of Mg-6 wt%Zn alloy during equal-channel angular pressing // *Metals*. 2018. Vol. 8. № 10. Article number 841. DOI: [10.3390/met8100841](https://doi.org/10.3390/met8100841).
29. Dumitru F.-D., Higuera-Cobos O.F., Cabrera J.M. ZK60 alloy processed by ECAP: Microstructural, physical and mechanical characterization // *Materials Science and Engineering: A*. 2014. Vol. 594. P. 32–39. DOI: [10.1016/j.msea.2013.11.050](https://doi.org/10.1016/j.msea.2013.11.050).

## Изменение структуры, механических и коррозионных свойств сплава системы Mg–Zn–Zr, подвергнутого равноканальному угловому прессованию

© 2024

*Аксенов Денис Алексеевич*<sup>\*1,2,3</sup>, младший научный сотрудник  
*Фахретдинова Эльвира Илдаровна*<sup>1,2</sup>, кандидат технических наук, научный сотрудник  
*Асфандияров Рашид Наилевич*<sup>1,2,4</sup>, кандидат технических наук, научный сотрудник  
*Рааб Арсений Георгиевич*<sup>2,5</sup>, кандидат технических наук, научный сотрудник  
*Шарипов Арсений Елисеевич*<sup>2</sup>, магистрант  
*Шишкунова Мария Андреевна*<sup>2</sup>, аспирант  
*Сементеева Юлия Рамилевна*<sup>2</sup>, магистрант

<sup>1</sup>Институт физики молекул и кристаллов Уфимского федерального исследовательского центра РАН, Уфа (Россия)<sup>2</sup>Уфимский университет науки и технологий, Уфа (Россия)

\*E-mail: aksyonovda@mail.ru

<sup>3</sup>ORCID: <https://orcid.org/0000-0002-2652-2646><sup>4</sup>ORCID: <https://orcid.org/0000-0002-5522-4314><sup>5</sup>ORCID: <https://orcid.org/0000-0003-1993-413X>

Поступила в редакцию 05.06.2023

Принята к публикации 25.08.2023

**Аннотация:** Магниево-цинковые сплавы считаются перспективными материалами для изготовления биорезорбируемых имплантатов. Их основные недостатки – низкая прочность и коррозионная стойкость в биологических средах. В работе изучалось влияние интенсивной пластической деформации методом равноканального углового прессования (РКУП) на структуру, механические свойства и коррозионную стойкость магниевого сплава Mg–8,6Zn–1,2Zr. Установлено, что 1 цикл РКУП при 400 °С ведет к заметному упрочнению сплава Mg–8,6Zn–1,2Zr на ~10 %, до 330 МПа. Структурные исследования показали, что в трансформации структуры существенную роль играет динамическая рекристаллизация. РКУП ведет к формированию структуры бимодального вида с крупными деформированными зёрнами со средним поперечным размером 20±4 мкм и рекристаллизованными зёрнами со средним поперечным размером 6±2 мкм. Установлено, что с понижением температуры деформации до 250 °С происходит процесс деформационно-индуцированного распада пересыщенного твердого раствора. Электропроводность образца после РКУП при 400 °С составляла 29±2 % согласно International Annealed Copper Standard (IACS), в то время как 2 цикла РКУП при 250 °С ведут к повышению электропроводности до 32±2 % IACS. Методом электрохимической коррозии установлено, что 1 цикл РКУП при 400 °С приводит к незначительному снижению коррозионной стойкости исследуемого сплава по сравнению с исходным состоянием. Показано, что ток коррозии увеличивается с 24 до 32 мкА/см<sup>2</sup>, в то время как последующий цикл РКУП при 250 °С увеличивает ток коррозии более чем в 2 раза (до 57 мкА/см<sup>2</sup>).

**Ключевые слова:** сплавы системы Mg–Zn–Zr; Mg–8,6Zn–1,2Zr; магниево-цинковые сплавы; высокая прочность магниево-цинковых сплавов; РКУП; коррозионная стойкость; электропроводность; динамическая рекристаллизация при РКУП.



**Благодарности:** Работа выполнена при поддержке Российского научного фонда (грант № 22-79-10325, <https://www.rscf.ru/project/22-79-10325/>).

Статья подготовлена по материалам докладов участников XI Международной школы «Физическое материаловедение» (ШФМ-2023), Тольятти, 11–15 сентября 2023 года.

**Для цитирования:** Аксенов Д.А., Фахретдинова Э.И., Асфандияров Р.Н., Рааб А.Г., Шарипов А.Е., Шишкунова М.А., Сементеева Ю.Р. Изменение структуры, механических и коррозионных свойств сплава системы Mg–Zn–Zr, подвергнутого равноканальному угловому прессованию // Frontier Materials & Technologies. 2024. № 1. С. 9–17. DOI: 10.18323/2782-4039-2024-1-67-1.